Ship collision analysis with a floating offshore fish farm

Zhaolong Yu & Jørgen Amdahl
Department of Marine Technology, Norwegian University of Science and Technology (NTNU), Norway
Center for Autonomous Marine Operations and Systems (AMOS), Norwegian University of Science and Technology (NTNU), Norway
David Kristiansen
SINTEF Ocean, Norway

ABSTRACT: Due to limited nearshore areas and great impact to local ecosystems, the aquaculture industry is moving the fish farms from nearshore to more exposed sea regions where waves and current are stronger. Like other offshore installations operating at sea, fish cages are also exposed to the risk of collisions from attendant or visiting vessels. This paper evaluates the structural strength of a fish farm concept subjected to supply vessel collisions by the use of nonlinear finite element simulations. The fish cage is made of ring-stiffened columns and supporting braces. A 7500-ton supply vessel is used as the striking vessel. Several collision scenarios with both coupled and decoupled methods are simulated on representative impact locations. The results are discussed with respect to the impact resistance, energy and structural damage.

1 INTRODUCTION

With the fish farming industry producing farmed Atlantic salmon going into more exposed seas, the cages become larger and much more fish can be accommodated than ever before. However, harsher environmental loads and frequent aquaculture operations imply risk for accidental actions, such as ship collisions, where the damage potential and possible consequences can be severe due to large units. Like other offshore installations e.g. jackets and jack-ups (Yu and Amdahl, 2018), submersible platforms (Skallerud and Amdahl, 2002) and wind turbines (Biehl and Lehmann, 2006), fish farms are exposed to the risk of collisions, both from service vessels and merchant vessels on erroneous track. This may represent a major threat to the safety and integrity of the fish farms. A major collision may cause extensive structural damage and in the extreme cases, the fish farm may collapse completely with fish escape as a result. Escape of farmed fish is considered to have negative impact on the wild stocks and will cause major economic losses for the fish farming company. More seriously, a collision event may also represent a safety threat for the personnel both on the ship and the fish farm. Hence, this should be avoided by proper safety measures to reduce the likelihood of collision and by direct design or by a combination. However, design aspects of accidental loads from ship collisions are not included in the present Norwegian technical standard for design of fish farms [Standards Norway NS 9415:2009].

Loads due to intended interactions during regular aquaculture operations in moderate sea-states with a well boat moored next to a conventional fish cage, can be significant for the fish farm structure (Shen et al., 2019). To increase the operational window, new concepts for offshore fish farming often rely on contact free operations between service vessels or cargo vessels and the fish farm, as for reception of feed supplies. However, frequent operations involving the close maneuvering of ships by a fish farm in most weather conditions implies risk of collision. Collision with other vessels is also a realistic scenario, and the probability of close passing by merchant vessels can be estimated from automatic identification system (AIS) data (Aarsæther and Moan, 2009).

In addition to resisting the direct actions during collision, the damaged structure should maintain sufficient residual strength so that it can resist operational and environmental loads before it can be repaired. Realistic estimates of the environmental load levels at a given site and structural condition rely on adequate descriptions of the marine environment, including the exposure to wind, waves and current , see e.g. Bore and Amdahl (2017) and Kristiansen et al. (2017).

Ship collision has been considered for many decades in the offshore industry. In the design against ship collision actions, the kinetic energy of the vessel is determined by a risk assessment. Alternatively, current practice in the North has been to consider impact from a supply vessel of 5000 tons with a kinetic energy of 11 MJ for bow or stern impact and 14 MJ for sideway impact. These standard values were increased to 50 MJ and 28 MJ in the revised standard for offshore structures NORSOK N-003 standards.

At present, standard collision actions are not established. The intention of this work is to investigate the resistance to collision and permanent damage of a selected fish farm as a function of the collision energy or the impact speed. No comparison is made with acceptance criteria as they have generally not been established. It is emphasized that structural damage is investigated only, penetration of the net may occur for small impact energies, and the potential of fish escape can be large, even if integrity of the structure is not put in jeopardy.

For practical reasons, the striking vessel selected is a 7500-ton offshore supply vessel, which is larger than typical fish harvesting vessels and well boats, but it is not out of range. Thus the analysis results are conservative with respect to safety considerations of the fish cage. The fish cage model, the striking supply vessel model and the collision scenarios are described in detail. The nonlinear finite element code LS-DYNA 971 is used for the numerical simulations. The local strength analysis studies only the relatively weak columns 1, 3, 5, 7 and 9. Future work could be extended to cover the local strength analysis of column 2, 4, 6, 8 and 10.

2 MODEL DESCRIPTIONS

2.1 *The striking supply vessel*

A modern standard supply vessel bow is used in the study. The principal dimensions of the vessel are given in Table 1. The bow model is shown in Fig. 1. The element size is generally 120 mm. The plate thickness varies from 7 mm for the decks to 12.5 mm in the bulb. The stiffener spacing is approximately 600 mm, with ring stiffeners and breast hooks of approximately 250 × 15 mm in the bulb. The bulbous part is almost cylindrical and is relatively strong. The forecastle protrudes 1.2 m ahead of the bulb.

Table 1. Principal dimensions of the striking vessel

Displacement	7500	ton
Length	90	m
Breadth	18.8	m
Depth	7.6	m
Draft	6.2	m

Both decoupled and coupled simulations are carried out. For the coupled simulation including ship global motions and hydrodynamic forces, the implementation is fulfilled using the user defined load subroutine in LS-DYNA, and a detailed description of the coupled simulation procedures are given in Yu et al. (2016b), Yu et al. (2016a) and Yu and Amdahl (2016). Verification has been carried out where the collision forces are extracted from LS-DYNA simulations and applied to the motion solver SIMO (Marintek, 2012) considering the linear potential flow theory. The motions measured from LS-DYNA simulation compared reasonably with SIMO results, demonstrating good accuracy of the implementation.

For coupled simulations, the ship's hull girder is represented by a long rigid beam from the bow back towards the center of gravity of the vessel; see Fig. 2. The rigid beam and the deformable ship bow are connected to a rigid shell plate at the rear of the bow model. The beam properties are calibrated to represent correctly the total mass and inertia of the ship with respect to the center of gravity taking into account the contribution of the bow model. The 6DOF hydrodynamic forces and moments are applied as user-defined loads at the COG of the ship. Because the user defined load subroutine does not allow applying bending moments directly, the bending moments have to be transformed into force pairs. Therefore, several small rigid beams are created for applying bending moments in roll, pitch and yaw. The interaction of the beams is located at the center of gravity (see Fig. 2).

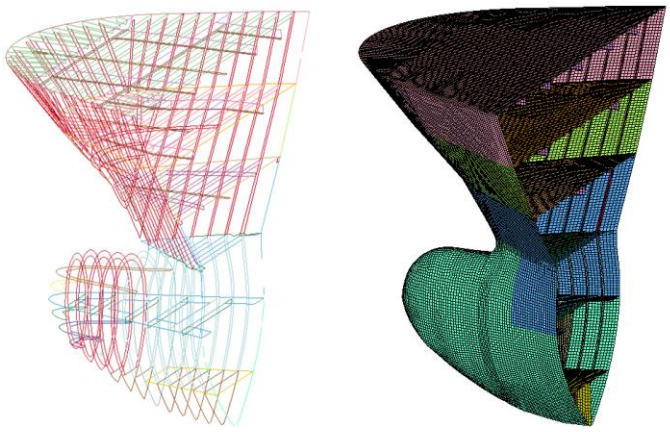

Fig. 1. The FE model of the bulbous bow

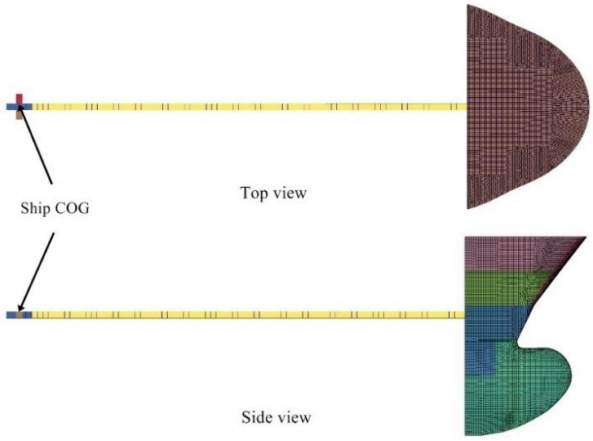

Fig. 2. The FE model of the striking ship

2.2 *The fish cage model*

The floating fish cage consists of many ring-stiffened tubes and columns that constitute a space frame. The cage is slack-moored at sea. It has a diameter of 110 m and is designed to accommodate 1.5 million salmons. The finite element model of the

whole fish cage is illustrated in Fig. 3, which is the model used by USFOS software for global response analysis.

Focus is placed on local strength assessment using a detailed shell finite element modelling. The selected part for the local analysis is indicated by the dashed line in Fig. 3. The local model is given in Fig. 4. The middle column is 35.1 meters in height with a column diameter of 2.75 m. The column outer shell thickness varies from 23 mm to 40 mm as shown in Fig. 4. The columns are equipped with ring stiffeners T300×200×10×15, which are arranged every 3 m. The connecting transverse tube is 2.25 m in diameter and the tube thickness varies from 19 mm to 40 mm as shown in Fig. 4. Ring stiffeners with dimensions of T300×200×10×15 are arranged every 3.2 m. Finite element models of the ring stiffeners are shown in Fig. 5.

The numerical simulation is carried out by using the explicit finite element software LS-DYNA 971. The four-node Belytschko-Lin-Tsay shell element is used. The shell element size is in general 100 mm, which is typically adopted in ship collision analysis. More refined meshes are used for the ring stiffeners and stringers. Five elements are used for the stiffener web and four elements are for the stiffener flange, and this is considered sufficient to develop buckling modes (see Fig. 5).

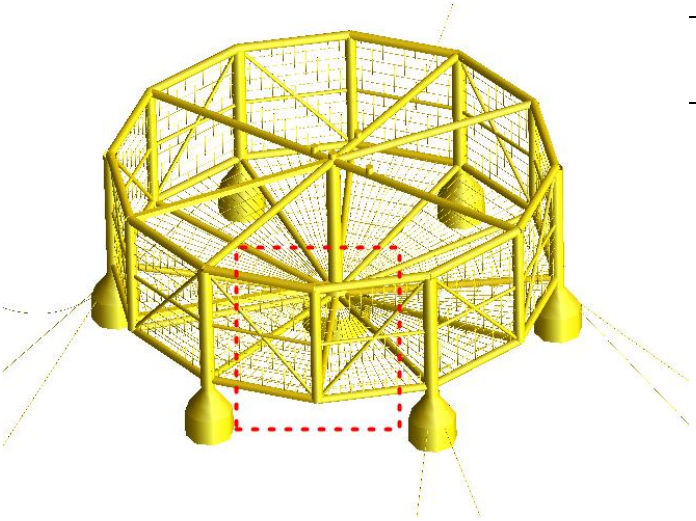

Fig. 3. The fish cage model in USFOS using beam elements

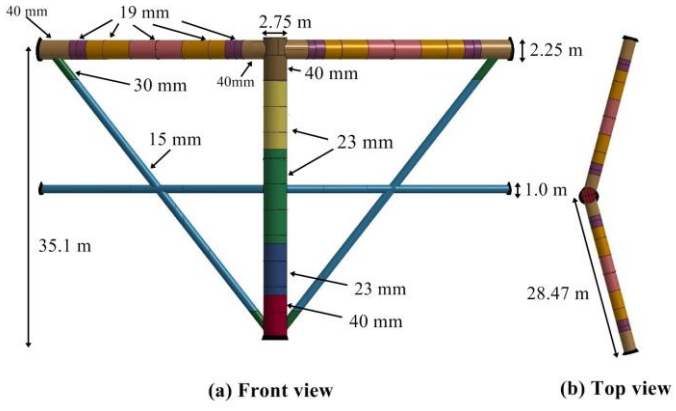

Fig. 4. The detailed shell element model for the local column

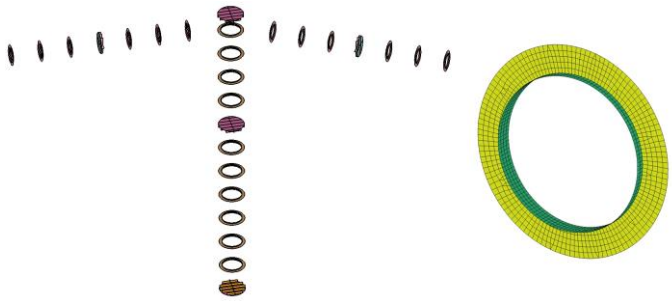

Fig. 5. Finite element model of ring stiffeners

2.3 *Material modelling*

When ship-structure interactions are accounted for, proper modelling of the material behavior is essential because relative strength of the striking and struck objects are very sensitive to material strength and failure. A rupture of structures can easily turn the strong structure into the weak.

The power law hardening model is used to accurately model the plastic strain hardening for steel, and a yield plateau is defined to delay the onset of hardening. The steel material property used for modelling the ship and the fish cage are given in Table 2. The state-of-art Rice-Tracey-Cockcroft-Latham (RTCL) damage criteria (Tørnqvist, 2003) is used to model fracture.

Table 2. Material properties for the ship and brace/leg models

Material	*Density(kg/m^3)*	*σ_y (Mpa)*	*E (Gpa)*	*K (Mpa)*	*N*	*$\varepsilon_{plateau}$*
supply vessel	7850	275	207	830	0.24	0.01
fish cage	7850	355	207	780	0.22	0.00

2.4 *Collision scenarios*

2.4.1 *Decoupled simulations*

Three collision scenarios are analyzed for decoupled simulations as shown in Fig. 6.

Scenario 1: Bow collision with the column

Scenario 2: Bow collision with the middle of the transverse supporting tube

Scenario 3: Bow collision with one quarter span of transverse supporting tube and diagonal braces for scenarios

The relative position of the ship and the fish cage is adjusted according to the operational draft of both structures. The ends of the column, the supporting tubes and the supporting braces are fixed against all degrees of freedom motions. The boundaries are marked in black in Fig. 4. The striking ship is assumed to move with a prescribed velocity of 3 m/s. The penalty based contact algorithms are used to model the contact between the vessel and fish cage structure, and the internal contact of the ship and the fish cage itself. A friction coefficient of 0.3 is assumed for all the contacts.

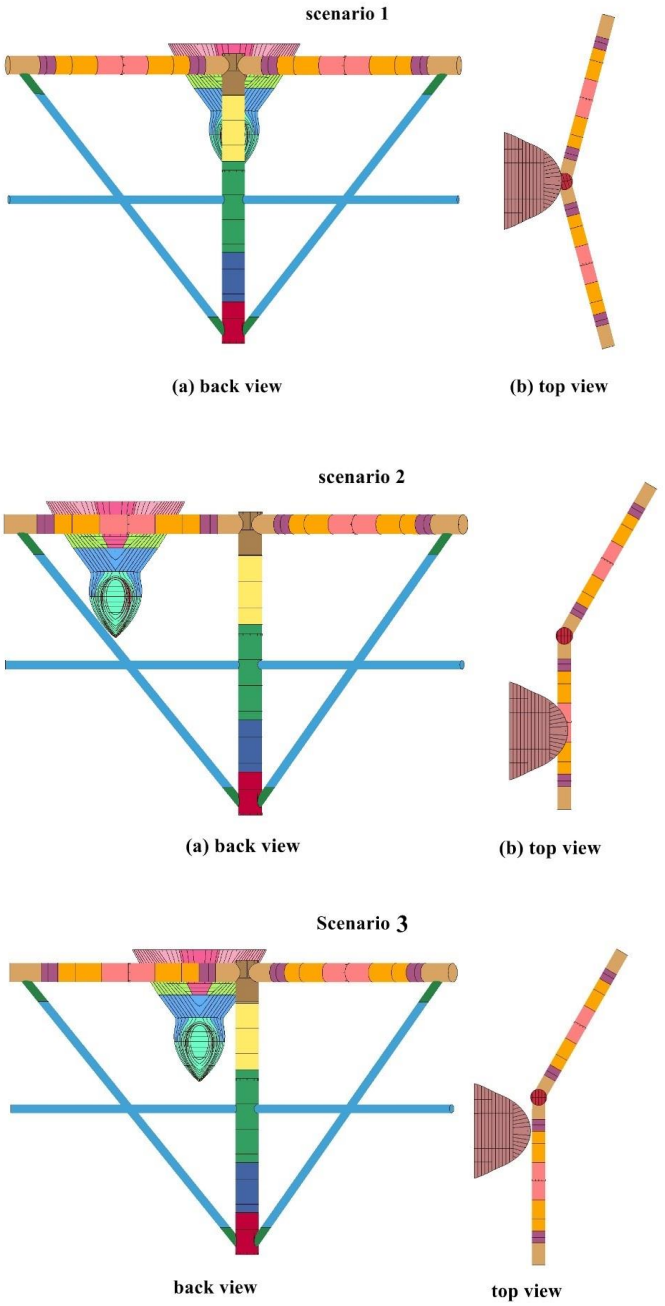

Fig. 6. The collision scenarios for decoupled simulation

2.4.2 *Coupled simulations*

A scenario 4 is established for the coupled collision analysis in Fig. 7. The collision angle is $\alpha=60^{\circ}$. The relative position of the ship and the fish cage is adjusted according to the operational draft of both structures. The ends of the column, the supporting tubes and the supporting braces are fixed against all degrees of freedom motions. The striking ship is given an initial velocity of 3 m/s. The penalty based contact algorithms are used to model the contact between the vessel and fish cage structure, and the internal contact of the ship and the fish cage itself. A friction coefficient of 0.3 is assumed for all the contacts.

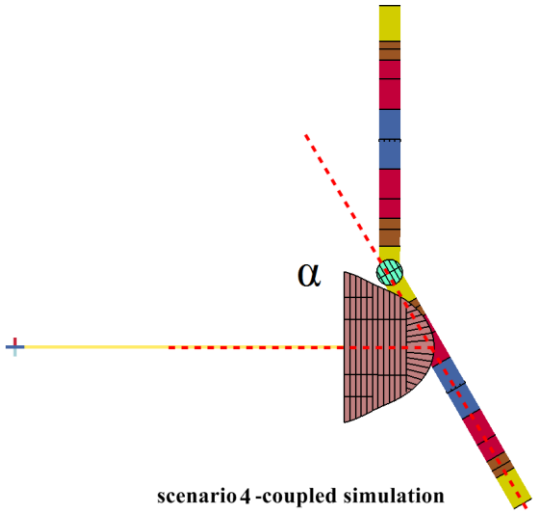

Fig. 7. The collision scenario for coupled simulations

3 DECOUPLED SIMULATION RESULTS AND DISCUSSIONS

3.1 *Collision scenario 1*

In this scenario, the supply vessel collides with the main column as shown in Fig. 6. The resulting energy dissipation and collision resistance are shown in Fig. 8. A total energy of about 31 MJ is dissipated for a total ship displacement of 2.8 m where initial fracture occurs. The total displacement of the ship equals the sum of the deformation of the ship bow and the deformation of the cage.

The collision forces for the stem and bulb attain a peak after 1.6 m displacement and then drop drastically. The energy dissipation before the drop is around 16.3 MJ. Up to this point, the column deformation is generally local. The column top with a stiffened top plate is quite strong and is able to crush the ship stem as shown in Fig. 9. At the lower contact point, the ship bulb is strong and crushes the column with minor bulb deformation while the column undergoes local denting. The sudden drop of forces is due to initiation of local buckling as shown in Fig. 10. This eases the contact between the ship stem and the top column plate. Considering the high diameter/thickness ratio (= 118), this is expected. According to ISO 19902 standard for fixed steel offshore structures, the ultimate bending moment capacity of the cross-section corresponds to first yield only, and the cross-section is thus not capable of developing a plastic hinge. Local buckling forms at the junction of shell a' (40 mm) and shell b' (19 mm); refer to Fig. 4. The whole structure starts to deflect globally. As the local buckle develops, the bending moment and the collision force level drop.

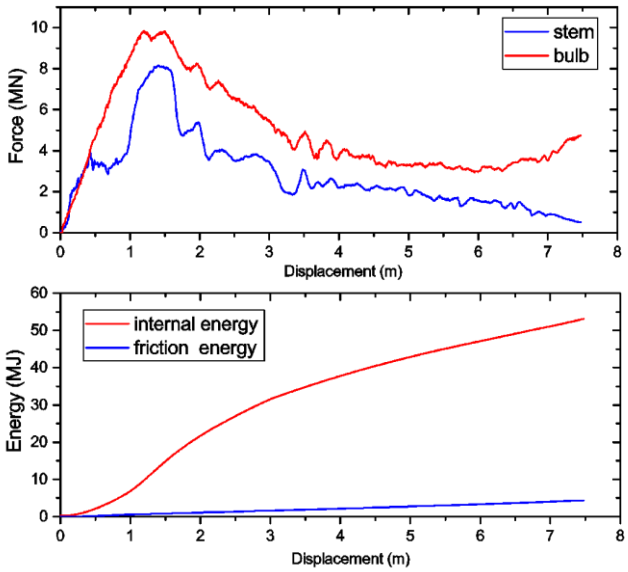

Fig. 8. Collision energy and resistance for collision scenario 1. The displacement is measured as displacement of the ship hull and includes deformations of the bow as well as the structure.

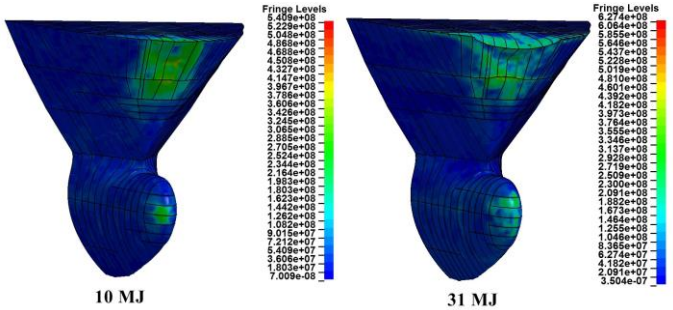

Fig. 9. The ship bow deformation after a total energy dissipation of 10 MJ and 31 MJ

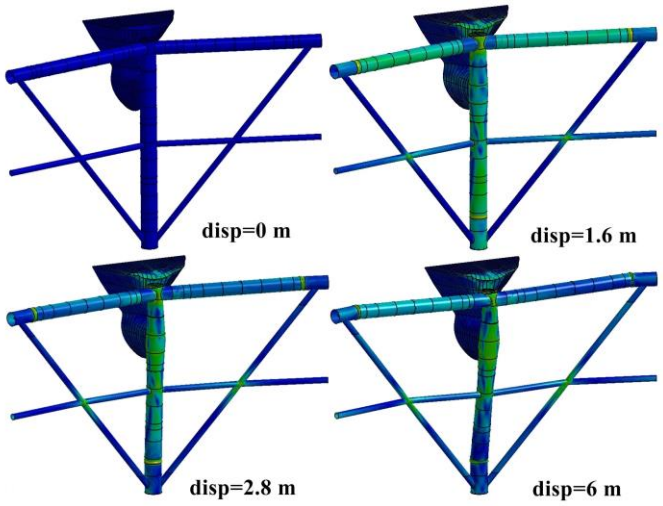

Fig. 10. Structural deformations at different total displacements

As the deformation continues after initial buckling, the lateral deflection of the column increases significantly. For a total energy dissipation of approximately 31 MJ corresponding to a displacement of 2.8 m, the left end of the transverse supporting tube undergoes fracture initiation as shown in Fig. 11. At this stage, it is interesting to find that fracture occurs on the compression side of the transverse tube. This is due to progressive buckling of the tube, causing bending fracture failure. The crack on the compression side does not propagate a lot and a considerable resistance maintained after initial fracture.

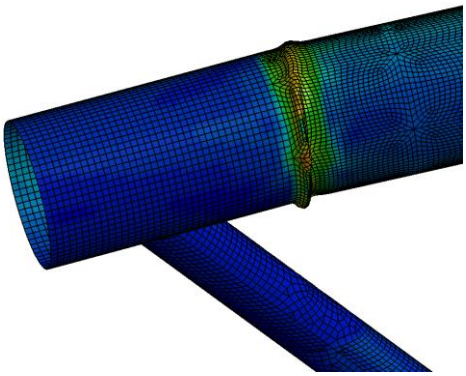

Fig. 11 Fracture of the left end of the transverse supporting tube at a displacement of 2.8 m

3.2 *Collision scenario 2*

In collision scenario 2, the ship stem hits the middle of the transverse supporting tube. The collision resistance and the internal energy are plotted in Fig. 12. It shows that the structure can absorb about 8.2 MJ before initiation of fracture at a displacement of 1.5 m. This energy is much lower than the value in scenario 1. However, because fracture due to progressive buckling is on the compression side, the crack does not propagate very fast and the structure still preserves considerable capacity. From the resistance and energy curves in Fig. 12, final collapse occurs at a total displacement of 7.0 m corresponding to a total energy of 40 MJ. The ships undergoes little damage during collision, and most of the energy is dissipated through deformation of the cage.

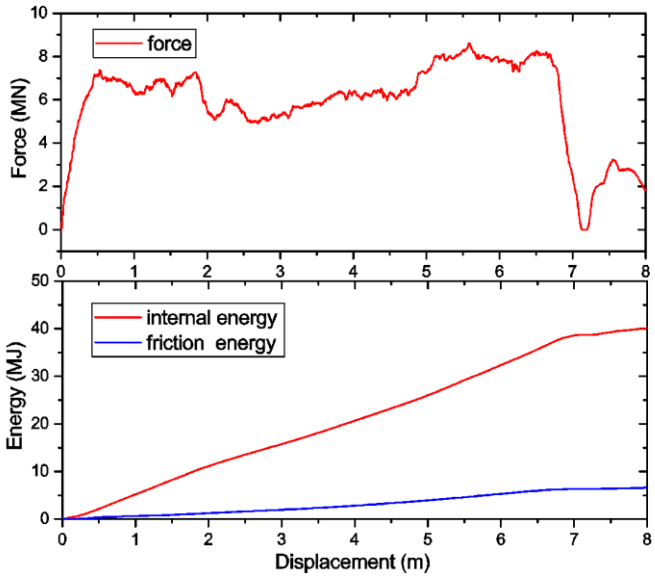

Fig. 12. collision energy and resistance for scenario 2

Fig. 13 shows deformation of the fish cage at different total displacements. For a total displacement

of 1.5 m, local buckling occurs at the shell connection with the thickness shifting from 19 mm to 40 mm. As the collision continues, buckling occurs in more places including the transverse tube on the right side and the main column. The buckled cross section is shown in Fig. 14. The buckling at the intersection of the main column and the diagonal braces seems to be induced by torsional moments.

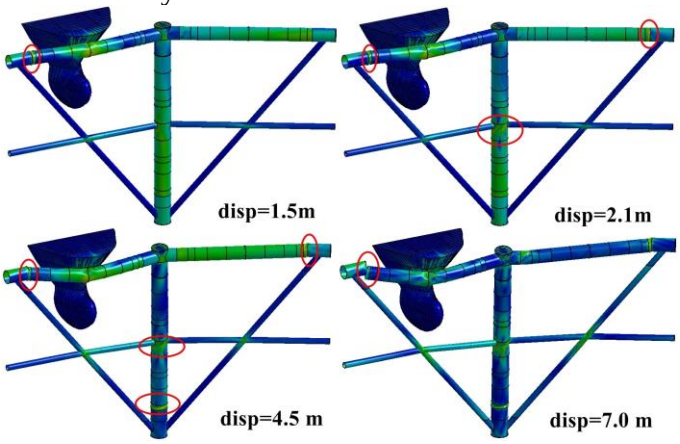

Fig. 13. Deformation of the fish cage at different total displacements

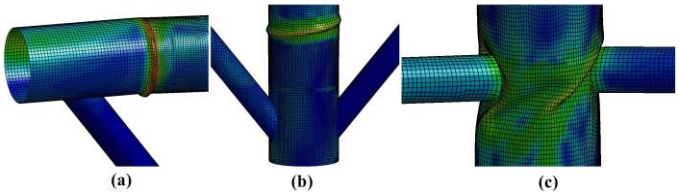

Fig. 14. Local buckling of the tube cross section

3.3 *Collision scenario 3*

In collision scenario 3, the ship crushes a quarter of the transverse supporting tube without hitting the braces. The collision resistance and internal energy are shown in Fig. 15. Initial fracture occurs at a displacement of 2.4 m corresponding to an energy dissipation of 14 MJ. As fracture occurs on the compression side due to progressive buckling, the crack does not propagate fast and considerable capacity is retained. From Fig. 15, the structure can absorb around 40 MJ at a displacement of 8.0 m without completely collapse. However, such large displacements should be avoided in order not to penetrate into the cage, causing fish escape.

The deformation of the fish cage structure at different total displacements is shown in Fig. 16. The structural responses are quite similar with scenario 2. When the ship moves 1.2 m into the fish cage structure, initial local buckling occurs on the left side of the transverse tube corresponding to an energy dissipation of 5.5 MJ. As the collision continues, buckling occurs at several places similar to the scenario 2.

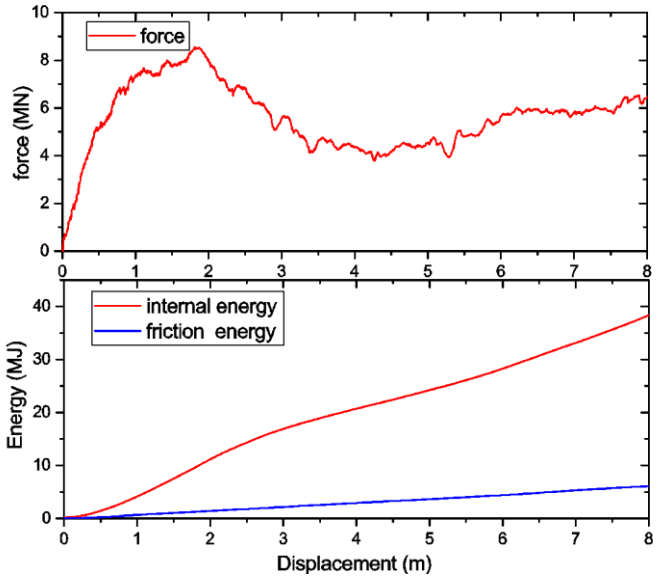

Fig. 15. Collision energy and resistance for scenario 3

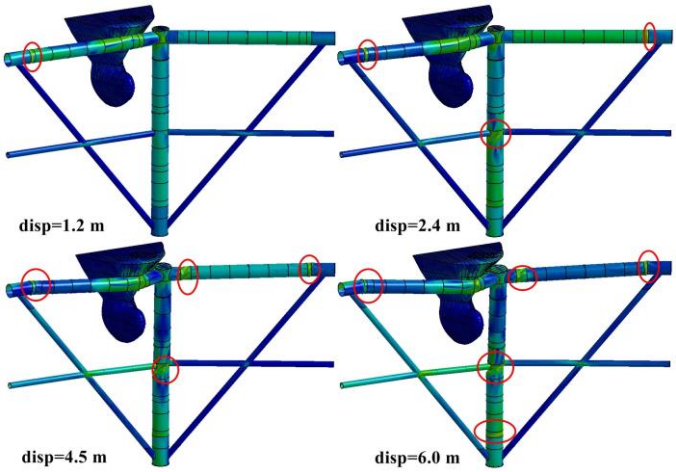

Fig. 16. Deformation of the fish cage for different dissipated energy levels

4 COUPLED SIMULATION OF COLLISION

The scenario 4 is simulated using the coupled solver considering hydrodynamic loads and ship motions. The initial collision angle is 60°. The collision force components are plotted in Fig. 17 and show that the collision lasts for about 7.5 s, which is relatively long and comparable to ship natural periods. All three force components are significant. Fig. 18 shows a side view of the ship with motion trajectories plotted for the bow and at the ship center of gravity. The temporal variation of the vertical displacement is plotted in Fig. 19. The plots show that the pitch and heave motions are significant. The ship bow moves a maximum of 1.15 m upwards, while the maximum heave displacement at the ship center of gravity is 0.25 m.

Fig. 20 shows a top view of the ship motion and structural damage. The sway and yaw motions are indicated and the time histories are plotted in Fig. 21. The plots show that the yaw angle is small because,

the tube deforms and tends to "wrap" around the ship stem after some time and lock the ship with respect to yaw motion. This can be evidenced by the Y force in Fig. 17, which changes sign after around 1.2 s.

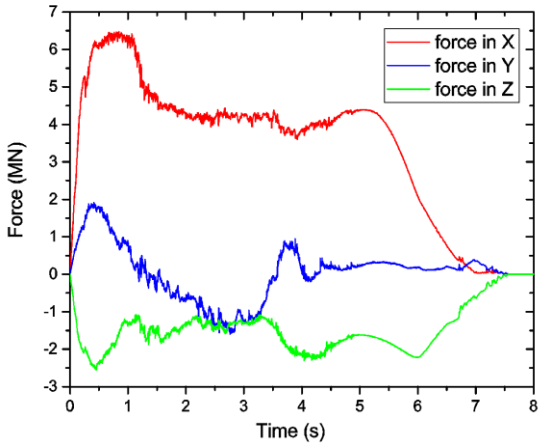

Fig. 17. The time variation of the collision forces

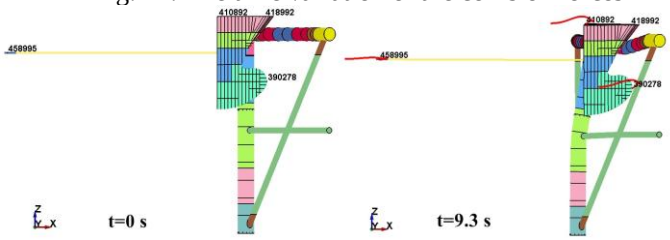

Fig. 18. A side view of the ship motions trajectories

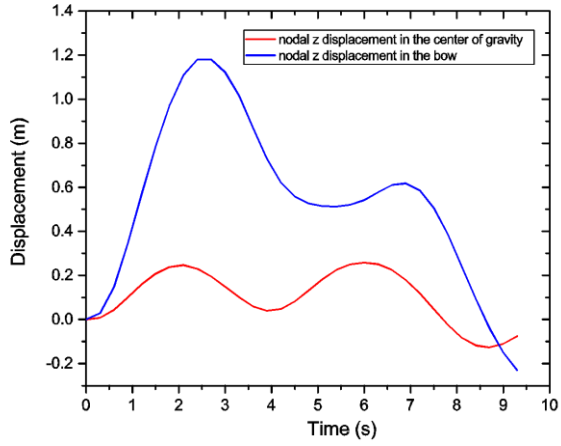

Fig. 19. The nodal vertical displacements at the center of gravity and the bow

The temporal variation of the internal energy and the friction energy is plotted in Fig. 22, and the energy is compared with external dynamic models by Liu and Amdahl (2010). The plots show the 3DOF external dynamic model underestimates the energy dissipation while energy predicted by the 6DOF model is even lower. This is mainly because ship motions are locked to extent due to tube deformations. The collision duration is long with complicated ship trajectories. During the process, the normal vector of the contact surfaces change significantly. In this case, the simplified external mechanics models may give inaccurate predictions and yield unconservative results. More discussions regarding the limitations of the external dynamic models can be found in Yu et al. (2019). It should however be noted that the present simulation disregards motions of the fish cage. In practice, the fish cage may be pushed away to some extent and release the contact, and thus the structural energy dissipation will be less.

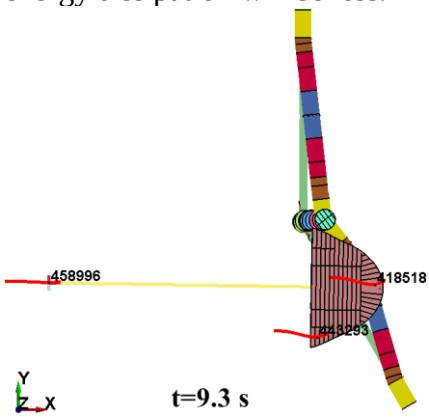

Fig. 20. A top view of ship motions during the collision

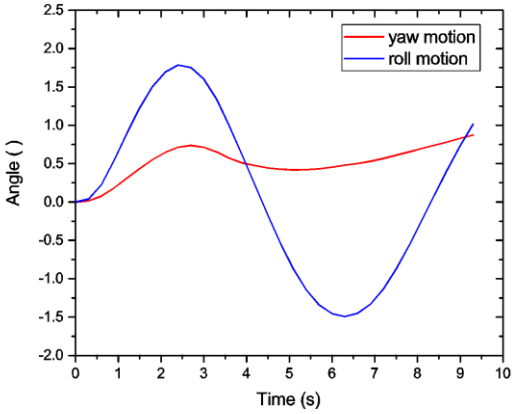

Fig. 21. The yaw and roll motion with time

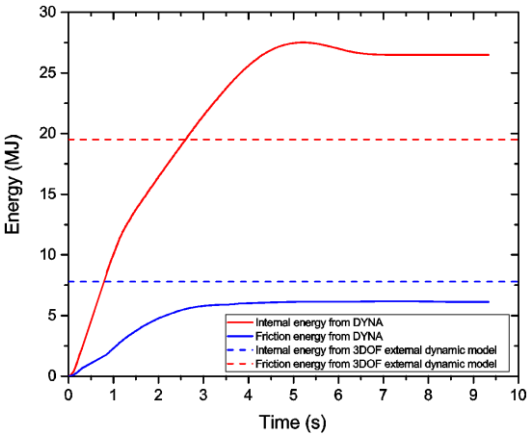

Fig. 22. Internal and friction energy from LS-DYNA and the external dynamic model

5 CONCLUSIONS

The local strength of the fish cage was analyzed the using nonlinear finite element code LS-DYNA. Four different collision scenarios were simulated. It is found that the most critical scenario is when the ship hits the middle of the transverse supporting tube, which undergoes initial fracture at an energy absorption of 8.2 MJ and collapses after a total internal energy dissipation of 40 MJ. In scenarios 1 and 4, the fish cage column undergoes severe deformations, but does not collapse completely after a displacement of 7.0 m and associated energy absorption of more than 40 MJ. The transverse supporting tube is relatively vulnerable to collisions, and for all the collision scenarios, fracture initially occurs on the transverse tube. The maximum force the transverse supporting tube can take is 6-7 MN. The energy levels listed are *internal energy*; some collision energy will remain as kinetic energy of ship and structure. A single global analysis indicate remaining energy could be in the range of 20%, so the critical collision energy will be larger approximately 20% larger. The scenarios are also a worst case scenario in the sense that the collision takes place normal to the cage, so the ship will not be pushed away (sway and yaw) from the farm.

During collision, local buckling occurs at several locations, typically at the joints with a significant change of plate thickness. The braces are generally thin-walled and susceptible to local buckling or denting. This limits the energy that the braces can dissipate by plastic bending or by the ship bow.

The coupled simulation captures the complicated ship motions with a long collision duration during the ship-fish cage collision. The pitch motion is very important in the studied case, where the ship bow can move a maximum displacement of 1.15 m up. Simplified external mechanics model may give inaccurate results in this case because the ship motion is locked by the structural deformations.

REFERENCES

AARSÆTHER, K. G. & MOAN, T. 2009. Estimating navigation patterns from AIS. *The Journal of Navigation,* 62**,** 587-607.

BIEHL, F. & LEHMANN, E. 2006. Collisions of ships with offshore wind turbines: Calculation and risk evaluation. *Offshore Wind Energy*. Springer.

BORE, P. T. & AMDAHL, J. Determination of Environmental Conditions Relevant for the Ultimate Limit State at an Exposed Aquaculture Location. ASME 2017 36th International Conference on Ocean, Offshore and Arctic Engineering, 2017. American Society of Mechanical Engineers, V03BT02A043-V03BT02A043.

KRISTIANSEN, D., AKSNES, V., SU, B., LADER, P. & BJELLAND, H. V. 2017. Environmental Description in the Design of Fish Farms at Exposed Locations. V006T05A003.

LIU, Z. & AMDAHL, J. 2010. A new formulation of the impact mechanics of ship collisions and its application to a ship–iceberg collision. *Marine Structures,* 23**,** 360-384.

MARINTEK 2012. SIMO - User's manual Version 4.0 rev0. *Marintek Report*.

SHEN, Y., GRECO, M. & FALTINSEN, O. M. 2019. Numerical study of a well boat operating at a fish farm in long-crested irregular waves and current. *Journal of Fluids and Structures,* 84**,** 97-121.

SKALLERUD, B. & AMDAHL, J. 2002. *Nonlinear analysis of offshore structures,* Research Studies Press Baldock, Hertfordshire, England.

TØRNQVIST, R. 2003. *Design of crashworthy ship structures.* Technical University of Denmark Kgns Lyngby,, Denmark.

YU, Z. & AMDAHL, J. 2016. Full six degrees of freedom coupled dynamic simulation of ship collision and grounding accidents. *Marine Structures,* 47**,** 1-22.

YU, Z. & AMDAHL, J. 2018. A review of structural responses and design of offshore tubular structures subjected to ship impacts. *Ocean Engineering,* 154**,** 177-203.

YU, Z., AMDAHL, J. & STORHEIM, M. 2016a. A new approach for coupling external dynamics and internal mechanics in ship collisions. *Marine Structures,* 45**,** 110-132.

YU, Z., LIU, Z. & AMDAHL, J. 2019. Discussion of assumptions behind the external dynamic models in ship collisions and groundings. *Ships and Offshore Structures*.

YU, Z., SHEN, Y., AMDAHL, J. & GRECO, M. 2016b. Implementation of Linear Potential-Flow Theory in the 6DOF Coupled Simulation of Ship Collision and Grounding Accidents. *Journal of Ship Research,* 60**,** 119-144.